Available online at www.sciencedirect.com
SCIENCE DIRECT®
Thermochimica Acta 419 (2004) 267–274
thermochimica acta
www.elsevier.com/locate/tca

Miscibility and phase separation in blends of phenolphthalein poly(aryl ether ketone) and poly(ethylene oxide): a differential scanning calorimetric study

Sixun Zheng [a,*], Kangming Nie [b], Qipeng Guo [c]

[a] *Department of Polymer Science and Engineering, Shanghai Jiao Tong University, 800 Dongchuan Road, Shanghai 200240, PR China*
[b] *College of Chemistry and Chemical Engineering, University of Anhui, Hefei 230039, PR China*
[c] *Division of Chemical Engineering, The University of Queensland, Brisbane, OLD. 4072, Australia*

Received 11 November 2003; received in revised form 3 March 2004; accepted 3 March 2004

Available online 24 April 2004

Abstract

Miscibility and phase separation in the blends of phenolphthalein poly(aryl ether ketone) (PPAEK) and poly(ethylene oxide) (PEO) were investigated by means of differential scanning calorimetry (DSC). The PPAEK/PEO blends prepared by solution casting from *N*,*N*-dimethylformamide (DMF) displayed single composition-dependent glass transition temperatures (T_g), intermediate between those of the pure components, suggesting that the blend system is miscible in the amorphous state at all compositions. All the blends underwent phase separation at higher temperatures and the system exhibited a lower critical solution temperature (LCST) behavior. A step-heating thermal analysis was designed to determine the phase boundaries with DSC. The significant changes in the thermal properties of blends were utilized to judge the mixing status for the blends and the phase diagram was thus established.

Keywords: Phenolphthalein poly(aryl ether ketone); Poly(ethylene oxide); Miscibility; Phase separation; Thermal analysis

1. Introduction

Polymer blends have played the important roles in the development of new materials with designed properties during the past decades [1,2]. The properties of polymer blends depend on the mixing degree of constituent polymers, and it is essential to investigate the miscibility and phase behavior of blend systems [1,2].

Phenolphthalein poly(aryl ether ketone) (PPAEK) is a newly developed high performance polymer [3] and it has been used as the matrix of polymer composites due to its excellent mechanical and thermal properties. In the viewpoint of chemical structure, PPAEK can be taken as the modified poly(ether ether ketone) (PEEK), and its repeat unit is schemed as the following

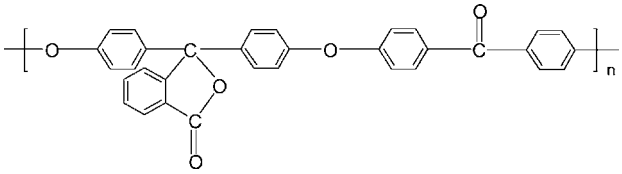

1.1. Phenolphthalein poly(aryl ether ketone)

The introduction of the rather bulky and polarizable phenolphthalein group in place of aromatic ring results in an increased rigidity of molecular chain, thus the much higher glass transition temperature (∼223 °C) than PEEK was displayed. Owing to the presence of the bulky phenolphthalein moiety, this polymer is no longer crystallizable.

There have been several reports on PPAEK blends with several other polymers [4–10]. It is of great interest to study miscibility and phase behavior of PPAEK with poly(ethylene oxide) (PEO). Firstly, this system consists of a very rigid amorphous component (PPAEK) and a very

* Corresponding author. Tel.: +86-21-54743278; fax: +86-21-54741297.
E-mail address: szheng@sjtu.edu.cn (S. Zheng).

0040-6031/$ – see front matter © 2004 Elsevier B.V. All rights reserved.
doi:10.1016/j.tca.2004.03.002

flexible low-melting point polyether, PEO. The extremely high difference of glass transition temperatures ($\Delta T_g \approx 290\,^{\circ}C$) between the components motivates us to investigate the T_g-composition behavior of the blends. A theoretical framework to rationalize the glass transition behavior of binary blend systems with big T_g difference between component polymers was provided by the free volume theory proposed by Kovacs [11]. In the present system, it is expected that there will be a break in the T_g-composition curve since the free volume of the high T_g component tends to be zero [11]. Secondly, the effect of a miscible and rigid component (viz. PPAEK) on the crystallization of PEO is also of interest in the specific crystalline/amorphous blends.

Calorimetric approach has been demonstrated to be powerful to investigate miscibility and phase behavior of polymer blends. The measurement of de-mixing heat and determination of glass transition temperatures (T_g) by differential scanning calorimetry (DSC) have been satisfactorily employed to establish miscibility and phase diagram of amorphous polymer blends; the appearance of two separate T_g during the step-heating DSC scans can be taken as the onset of phase separation [1,2]. However, in crystalline polymer blends, it was generally difficult unambiguously to follow the appearance of separate T_g owing to the high crystallinity of crystalline component. Nevertheless, the evolution of other thermal properties, such as thermal enthalpies (ΔH_m, ΔH_c), melting temperature (T_m) and crystallization temperature (T_c) etc., of the crystalline component can alternatively be exploited to judge phase behavior of blends [12,13]. In this work, we report the study on miscibility and phase behavior of the crystalline PPAEK/PEO blends by means of calorimetric measurement; the miscibility, and phase separation will be addressed.

2. Experimental

2.1. Materials and preparation of samples

Phenolphthalein poly(aryl ether ketone) was supplied by Xuzhou Engineering Plastics Co., Xuzhou, China. It has a glass transition temperature (T_g) of c.a. 223 °C. Gel permeation chromatogram (GPC) measurement indicates that the polymer has the molecular weight of $M_n = 17,000$ and $M_w/M_n = 3.60$. Poly(ethylene oxide) was purchased from Shanghai Reagent Co., Shanghai, China, and it has a quoted molecular weight of $M_n = 20,000$.

The PPAEK/PEO blends were prepared by casting from tetrahydrofuran (THF) solution at room temperature and from *N*,*N*-dimethylformamide (DMF) at 50 °C, respectively. The total polymer concentration was controlled within 5% (w/v). To remove the residual solvent, all the blend films were further dried in vacuo at 60 °C for 2 weeks. The blends prepared via DMF solution casting were used throughout the work.

2.2. Measurement

The calorimetric experiments were performed on a Perkin–Elmer Pyris 1 differential scanning calorimeter in a dry nitrogen atmosphere. The instrument was calibrated with Indium standard. In order to measure glass transition temperature (T_g), all the amorphous samples (about 15 mg in weight) were first heated up to the temperatures between phase separation and glass transition and held for 5 min to remove the thermal history, followed by quenching to −70 °C. For the crystalline samples (about 10 mg in weight), the pre-treatment temperature was taken at 70 °C, which is above the melting point of PEO (c.a. 65 °C) and below the lower critical solution temperature (LCST) and the samples were quenched to −70 °C. A heating rate of 20 °C/min was used at all cases. Glass transition temperature (T_g) was taken as the mid-point of the heat capacity change, whereas melting temperature (T_m) and crystallization temperature (T_c) were taken as the maximum of endothermic peak and the minimum of exothermic peak, respectively.

Phase separation processes were investigated with the following step-heating procedure [12,13]. The samples were first annealed at a selected temperature for 10 min, and then quenched to −70 °C. After that, the heating scan was performed to next higher temperature at 20 °C/min and the sample was maintained at this temperature for 10 min, and quenched. The higher temperature was changed by 10 °C interval. This procedure was repeated until the occurrence of phase separation was observed. The temperatures of phase separation were taken as the annealing temperatures at which the thermal properties (e.g., T_g, T_c, T_m, ΔH_m, and ΔH_c) were dramatically changed.

3. Results and discussion

3.1. Miscibility of PPAEK/PEO blends

All the PPAEK/PEO blend films casting from THF were cloudy at room temperature and at elevated temperatures, suggesting that the blends were phase-separated, which was confirmed by DSC traces and the observation with optical microscope. However, the transparent films of PPAEK/PEO blends (PEO < 40 wt.%) were obtained when cast from DMF. Due to the formation of PEO spherulites, the blends with PEO content more than 40 wt.% are not transparent, which was evidenced by the fact that all the samples became transparent when heated up to 80 °C (above the melting point of PEO). The transparency indicates that the PPAEK/PEO blends present single, homogeneous, amorphous phase, i.e., no phase separation occurs at least on a scale exceeding the wavelength of visible light. When further heated up to 200 °C, however, all the initially clear blend samples became cloudy in succession. The careful observation with the phase-contrast microscope indicates the formation of phase-separated structure in the cloudy samples. This

observation suggests that the PPAEK/PEO blends display a critical solution temperature behavior.

It was noted that phase behavior of the blends is quite dependent on the selection of casting solvents. The "solvent effect" on the homogeneity of casting polymer blend films has previously been interpreted in terms of the difference between the two polymer–solvent interaction parameters $|\chi_{12}-\chi_{13}|$ or $|\Delta\chi|$ (herein subscript 1 referring to solvent whereas subscript 2 (or 3) standing for polymer). From a ternary phase diagram, a homogeneous system is attained only with a suitably small difference between interaction parameters $|\Delta\chi|$, and in addition, a small polymer–polymer interaction parameter χ_{23} is necessary [14–19]. The transparent blend films prepared via DMF were used throughout this study.

3.1.1. Glass transition behavior

All the blends were subjected to thermal analysis and the DSC curves were shown in Fig. 1. It can be seen that each blend displayed a single glass transition temperature (T_g), intermediate between those of the two pure components and varying with the blend composition. In view of the glass transition behavior, it is concluded that PPAEK/PEO blends are miscible in the amorphous state, i.e., possess single homogeneous, amorphous phases.

From Fig. 1, it is seen that for pure PEO, 10/90, 20/80 PPAEK/PEO blends, no cold crystallization transitions were observed since crystallization was sufficiently rapid and occurred to completion during the quenching. However, the DSC curves of the blends containing 70, 60, and 50 wt.% of PEO displayed cold crystallization phenomenon after glass transition and the crystallization temperatures (T_c) increased with increasing PPAEK content. This observation indicates that the crystallization of PEO becomes progressively difficult in PPAEK-rich blends. While PPAEK content is more than 50 wt.%, there is no melting transition of PEO in blends because the degree of supercooling (i.e., T_m–T_g) is almost nonexistent, i.e., the absence of significant supercooling restricts PEO from crystallization upon cooling from the molten state, i.e., the amorphous phase is rigid in the temperature range where PEO chains normally rearrange into the 7/2 helical conformation, which is required for crystallization to occur. In addition, the melting temperature (T_m) of PEO in the blends significantly depressed with addition of PPAEK to the system, suggesting a negative intermolecular interaction energy density (B_{12}) [20,21]. This is characteristic of miscible blends composed of an amorphous and a crystalline polymer in which the amorphous component possesses a much higher T_g. It was noted that the experimental T_m for the blends with higher PPAEK content (30, 40, 50 wt.%) were high than those with 10 and 20 wt.% of PPAKE. This result could be responsible for the reorganization of PEO crystal during DSC heating scan.

Fig. 2 shows the plot of crystallinity of PEO in the blends as a function of blend composition, which was calculated from the following equation

$$X_c = \frac{(\Delta H_f - \Delta H_c)}{\Delta H_f^0} \times 100\% \quad (1)$$

Where X_c is percent crystallinity. ΔH_f and ΔH_c are the enthalpy of fusion and crystallization of PEO, respectively. ΔH_f^0 is the fusion enthalpy of perfectly crystallized PEO, and has been reported to be 205 J/g [22]. The crystallinity of PEO in the blends containing PPAEK dramatically deviates

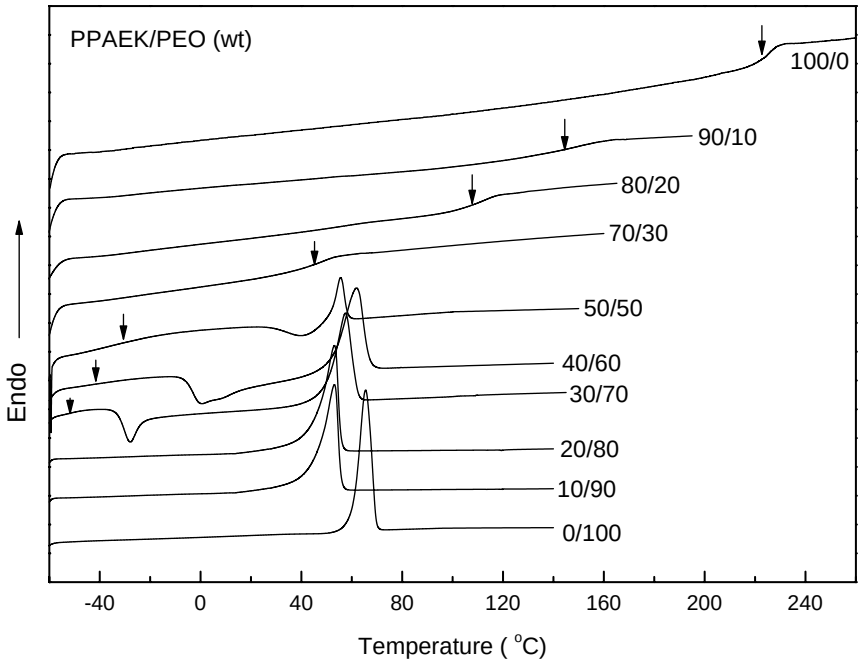

Fig. 1. DSC curves of PPAEK/PEO blends.

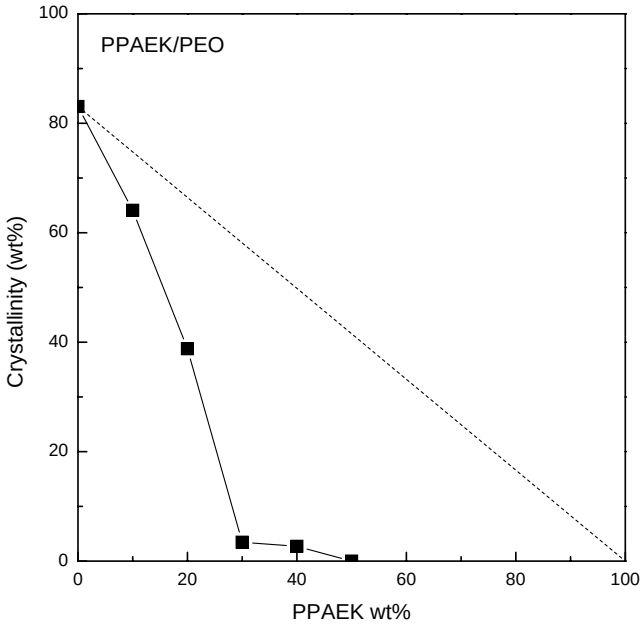

Fig. 2. Percent crystallinity of PEO in PPAEK/PEO blends. (■) The data were obtained from quenching 70 °C and rescanning at 20 °C/min; the dashed line represents the crystallinity of PEO in blends if the crystallization process were not influenced by the presence of PPAEK.

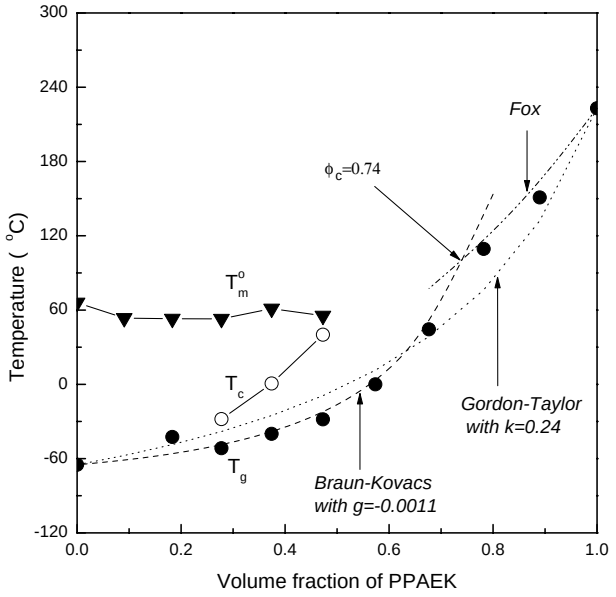

Fig. 3. Plots of thermal transition temperatures as functions of blend composition for PPAEK/PEO blends. T_g-composition relation analysis: (1) Fox equation; (2) Gordon–Taylor equation with $k = 0.24$; (3) Braun–Kovacs equation with $g = -0.0011$.

from the dashed line, which stands for the crystallinity of PEO in the blends if the crystallization process were not influenced by the presence of PPAEK, indicating a pronounced inhibition of crystallization by the presence of PPAEK. The supercooling of PEO crystallization decreased with increasing PPAEK contents in the miscible blends. The absence of significant supercooling will restrict PEO from crystallization upon cooling from the molten state; the amorphous phase is vitrified and thus crystallinity decreases dramatically with increasing PPAEK contents.

There are several theoretical and empirical equations to describe the dependence of glass transition temperature on blend composition. Among them the Fox [23] and the Gordon–Taylor [24] equations are mostly used. The Fox equation is shown below

$$1/T_g = W_1/T_{g1} + W_2/T_{g2} \tag{2}$$

where W_i is the weight fraction of component i and T_g is the glass transition temperature of blend, assuming that the specific heats of the two component are identical. For this system, Fox equation failed to fit the experimental T_g values in the entire composition. The Gordon–Taylor equation [24] was also applied to account for T_g-composition relationship of the system

$$T_g = \frac{W_1 T_{g1} + kW_2 T_{g2}}{W_1 + kW_2} \tag{3}$$

Where $k = \Delta\alpha_{p2}/\Delta\alpha_{p1}$, and $\Delta\alpha_{pi}$ is the difference in the thermal expansion coefficient between the liquid and glassy state at T_{gi}. The equation can describe the effects of thermal expansion on the T_g. In general, the k is an adjusting parameter related to the degree of curvature of the T_g-composition curve. Prud'homme and coworkers [25,26] proposed that in miscible polymer blends, the quantity k can be taken as a semi-quantitative measure of strength of the intermolecular interaction between components of polymer blends. The Gordon–Taylor fit to the data yielded a k value of 0.24 and however failed to reproduce the break observed in the T_g-composition variation (See Fig. 3).

These classical equations predict that T_g increase continuously (smoothly) and monotonically with blend composition. However, it was observed that the T_g-composition variation of several polymer blend systems is not monotonic and exhibits a cusp (or break) at the certain critical composition [27,28]. This phenomenon becomes very prominent when the T_g difference between the two homopolymers exceeds 50 °C. The classical equations become invalid below a critical temperature, T_{crit}, since the free volume of the high T_g component becomes zero. Kovacs [11] has proposed that the critical temperature, T_{crit}, and the critical composition, ϕ_{crit}, are given by

$$T_{crit} = T_{g2} - (f_{g2}/\Delta\alpha_2) \quad \text{if} \quad T_{g2} > T_{g1} \tag{4}$$

$$\phi_{crit} = \frac{f_{g2}}{\Delta\alpha_1(T_{g2} - T_{g1}) + f_{g2}(1 - \Delta\alpha_1/\Delta\alpha_2)} \tag{5}$$

where $\Delta\alpha_2$ is the difference between the volume expansion coefficients in the glass and liquid states of component 2 and f_{g2} is the free volume fraction of polymer 2 at T_{g2}. Below T_{crit}, the T_g of blend is described by

$$T_g = T_{g1} + \left(\frac{f_{g2}}{\Delta\alpha_1}\right)\left(\frac{\Phi_2}{\Phi_1}\right) \quad (6)$$

According to this equation, the blend T_g is uniquely determined by the properties of lower T_g component at temperature below T_{crit} or at composition below ϕ_{crit}. If there is excess volume between the two polymers upon mixing, Braun and Kovacs [29] have derived the following equations

$$T_g = T_{g1} + \frac{\Phi_2 f_{g2} + g\Phi_1\Phi_2}{\Phi_1\Delta\alpha_1} \quad (7)$$

where g is an interaction term defined as

$$g = \frac{(V_e/V)}{\Phi_1\Phi_2} \quad (8)$$

where V_e is the excess volume and V the volume of the blend. The excess volume (or g) is positive if blend interactions are stronger than the average interactions between molecules of the same species, and it is negative otherwise. Effectively, g is obtained by fitting the T_g-composition data to the Braun–Kovacs equation.

For the present blend system, the composition of the blends was expressed in terms of volume fraction (See Fig. 3). In the calculation, the density vales of 1.13 g/cm^3 for amorphous PEO [30] and 1.26 g/cm^3 for PPAEK were used, which was estimated by group contribution method [30]. The above three different equations were applied to account for the T_g-composition relationship. On the basis of the classical values of $f_{g2} = 0.025$ and $\Delta\alpha_2 = 0.00048\,K^{-1}$, the critical temperature and volume fraction (with respect of PPAEK) are obtained to be 440 K and 0.73, respectively. From Fig. 3, it is seen that Fox equation and Braun–Kovacs equation can well account for the T_g-composition dependence above and below ϕ_{crit}, respectively. The Braun–Kovacs fit yielded a g value of -0.0011. The negative value suggests that the blend interaction is fairly weak. It is seen that the crossover from the classical (Fox) limit to the free volume (Kovacs) regime occurred at about 0.74, which is satisfactorily close to the value of 0.73 predicted by Braun–Kovacs equation. It should be pointed out that at the high content of PEO (e.g., PPAEK/PEO 20/80 (wt.)), the T_g of the blend positively deviates from the predicted, which is due to the enrichment of the high-T_g PPAEK induced by crystallization of PEO [31–36].

3.2. Phase separation in PPAEK/PEO blends

At elevated temperatures, the PPAEK/PEO blends underwent phase separation. Such reversibility was a typical signature of lower critical solution temperature behavior. In this work, the LCST behavior was investigated by means of DSC and the step-heating method was employed to determine the phase boundaries, which was described in detail in Section 2. The annealing temperature corresponding to the first occurrence of the significant changes in thermal properties (e.g., T_g, T_m, T_c, ΔH_m, ΔH_c) was taken as the onset of phase separation [12,13]. It has been shown that the as-obtained phase diagram is identical with that obtained by laser scattering method [12].

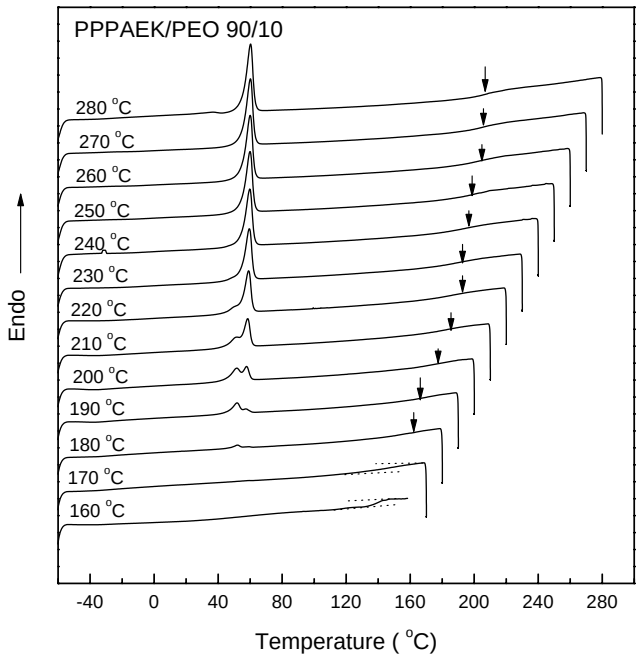

Fig. 4. Evolution of DSC curves after annealed at various temperatures between 150 and 280 °C for 10 min for PPAEK/PEO 90/10 (wt.) blend.

Depending on the blend composition, the changes in thermal properties during the step-heating DSC scans can display different features while phase separation occurs, which are respectively described as follows.

For the blends with PEO content less than 50 wt.%, no crystallinity was observed in the quenched samples. The evolution of thermal properties during the step-heating DSC scans for these blends can be representatively accounted for by PPAEK/PEO 90/10 (wt.) blend. After annealed at the specific temperature between 160 and 280 °C for 10 min and then quenched to −70 °C, a series of heating DSC curves for the blend were showed in Fig. 4. It can be seen that when annealed below 180 °C, the DSC scans show no obvious changes. However, the significant changes were observed, as the annealing temperature is higher than 180 °C. There appear minor melting transitions of PEO in the DSC heating thermograms, and the area under the melting peak increases with increasing annealing temperature, reaching a plateau when the annealing temperature is higher than 240 °C (See Fig. 5). It is seen that the melting temperature (T_m) increases with increasing the annealing temperature. The appearance of the crystallization of PEO in the blends is indicative of the occurrence of phase separation, i.e., the PEO-rich phase was formed from the initial homogeneous amorphous PPAEK/PEO mixture. With phase separation proceeding, PEO gradually concentrates from the original homogeneous blends and both the PEO-rich phase and PEO-lean phase are simultaneously formed, resulting in the appearance of the crystallization and fusion of PEO dur-

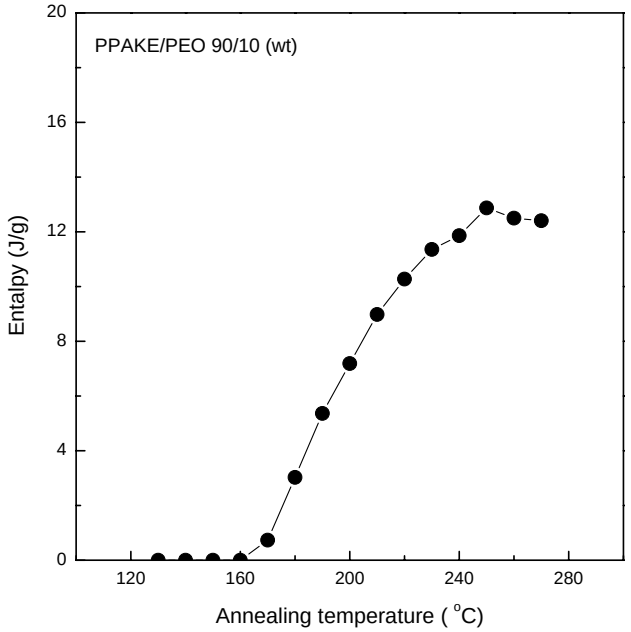

Fig. 5. Plot of PEO fusion enthalpy as a function of annealing temperature for PPAEK/PEO 90/10 (wt.) blend.

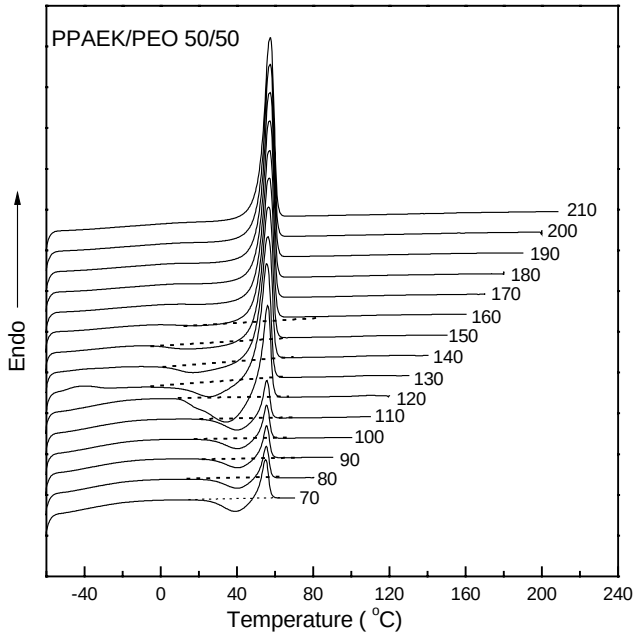

Fig. 6. Evolution of DSC curves after annealed at various temperatures between 70 and 210 °C for 10 min for PPAEK/PEO 50/50 (wt.) blend.

ing the process of quenching and heating run. The higher the annealing temperature, the larger the under the melting peaks, suggesting that the separation occurs more completely. Hence, the occurrence of the melting peak at a particular annealing temperature should be considered as the beginning of phase separation. From Fig. 4, it is observed that T_g of the blend became broad in the vicinity of the onset of phase separation. The width of the glass transition may reflect the magnitude of local compositional fluctuations in the polymer blends, implying the relative homogeneity or miscibility of the system. However, the transition temperatures do not change until the appearance of a minor melting peak in the DSC curve, indicating the occurrence of phase separation. With the phase separation occurring, the T_g gradually shift to higher temperature, although they increasingly became indistinguishable at higher annealing temperature due to its higher crystallinity after more complete phase separation. It is noted that the second T_g, i.e., that of the PEO-rich phase, cannot be seen in Fig. 4. It should be pointed out that the heating rescans after the appearance of the melting peaks of PEO does not show the cold crystallization of PEO, which indicates that the crystallization of PEO in the newly separated PEO-rich phase mainly occurs during quenching process. Similar cases were also seen for PPAEK/PEO 80/20, 70/30, 60/40 blends.

For PPAEK/PEO 50/50 blend, the amorphous mixture was obtained after quenching from 70 to −70 °C in terms of the comparison of the areas under the crystallization and melting peaks in the heating DSC curve. Fig. 6 shows a series of heating thermograms of the blend annealed between 70 and 210 °C. Below 120 °C, the endothermic enthalpy remains unchanged and equals to exothermic one, indicating that PEO crystallizes only during the heating run after quenching. When the annealing temperature is 110 °C or above, both the enthalpy values began to increase dramatically, and the enthalpy of fusion even began to surpass that of crystallization. At the same time, the cold crystallization temperatures (T_c) shifted to lower temperatures whereas the melting temperatures (T_m) increased (See Fig. 7). These results clearly display that, at annealing temperatures above 120 °C, PEO began to crystallize not only during the heating scan but also during the quenching process. In other

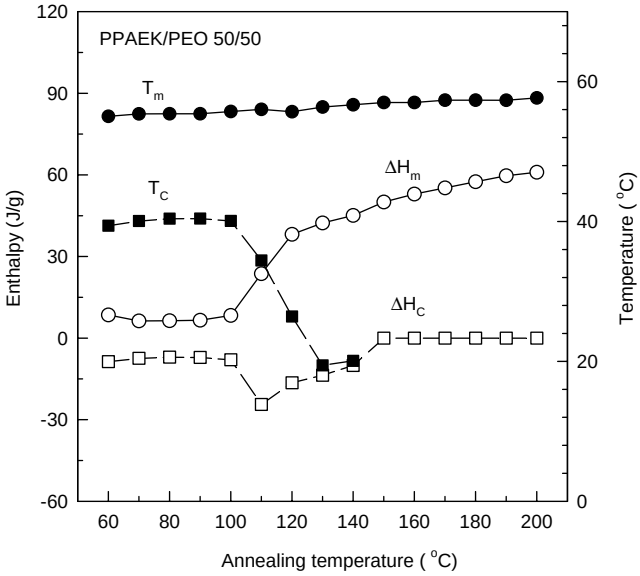

Fig. 7. Plots of thermal properties as function of annealing temperature for PPAEK/PEO 50/50 (wt.) blend.

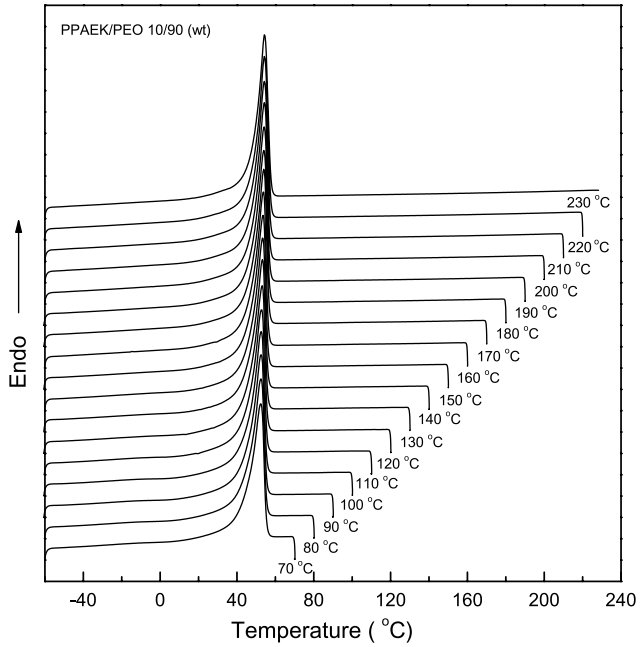

Fig. 8. Evolution of DSC curves after annealed at various temperatures between 70 and 190 °C for 10 min for PPAEK/PEO 10/90 (wt.) blend.

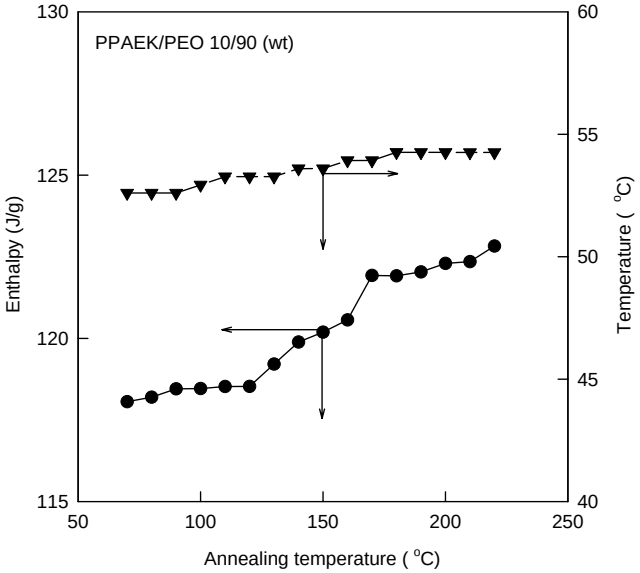

Fig. 9. Plots of thermal properties as function of annealing temperature for PPAEK/PEO 10/90 (wt.) blend.

words, on annealing, two separated amorphous phases are formed, i.e., one is the PPAEK-rich phase whereas the other corresponds to the PEO-rich phase. The PEO-rich phase can crystallize during quenching process. The cold crystallization of PEO becomes easier, i.e., the inhabitation effect of PPAEK on PEO crystallization reduces because the content of the amorphous component with higher T_g in the newly PEO-rich phase reduces. As a consequence, the enthalpy values of crystallization and fusion increased, and T_m increased since more perfect crystals could be formed. It is assumed that the shift of crystallization peak at a particular annealing temperature can correspond to the beginning of phase separation. It should be pointed out that annealing time is another important factor, which also affects the shift, and magnitude of crystallization peak after the phase separation occurs, whereas the parameters of thermal properties, such as enthalpy of fusion (ΔH_f), enthalpy of crystallization (ΔH_c), T_c, and T_m (See Fig. 7), remain constant before de-mixing during the step-heating DSC scans.

In the blends with PEO content more than 50 wt.%, PEO can crystallize during the quenching process. With increasing PEO content, the crystallization of PEO in the blends increasingly underwent to completion during the quenching. Representatively shown in Fig. 8 are a series of DSC curves of PPAEK/PEO 10/90 blend annealed at different temperatures ranging from 70 to 230 °C. The plot of thermal enthalpy of fusion and melting temperature as a function of annealing temperature is shown in Fig. 9. It is noted that, at or below 130 °C, the value of enthalpy almost remain constant, which indicates that the composition of the blends does not change during the annealing process, and namely the phase separation does not take place. However, when the annealing temperature is above 130 °C, enthalpy of fusion gradually increases with increasing annealing temperature, whereas the melting temperature increases. It is reasonable to believe that the changes of thermal enthalpy are caused by the occurrence of phase separation during annealing. Therefore, the phenomenon is indicative of the occurrence of phase separation. With increasing annealing temperature, the area under the melting peaks increased. When the annealing temperature is 130 °C or higher, the

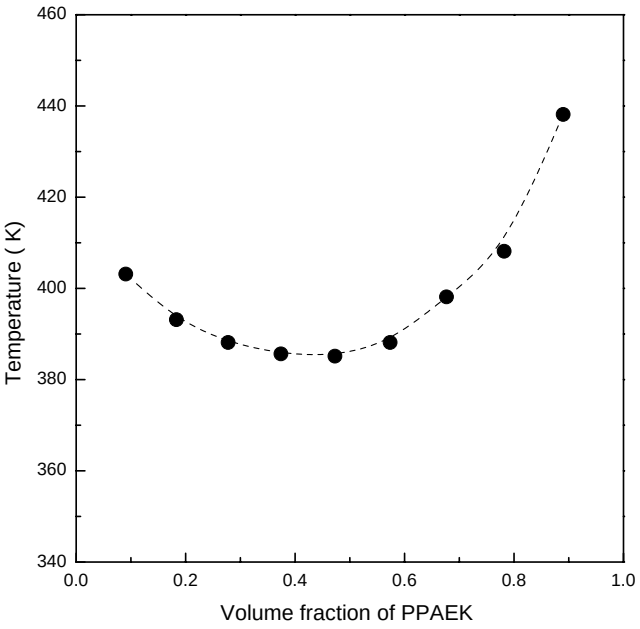

Fig. 10. Phase diagram of PPAEK/PEO blends: (●) the de-mixing temperatures determined by DSC.

thermal behavior is similar to that of pure PEO, suggesting that the phase separation has performed quite completely.

On the basis of the above-mentioned results of thermal analysis, the phase boundary diagram was established as shown in Fig. 10. The asymmetrical phase diagram has the minimum around 50 wt.% PEO and the system exhibits a typical lower critical solution temperature behavior.

4. Conclusions

The miscibility and phase behavior in semi-crystalline blends of PPAEK and PEO were investigated by differential scanning calorimetry. The blends are completely miscible in the amorphous state over the entire composition range at temperature $T < T_{cnf} = 109\,^{\circ}C$ from the transparency of blend films and the glass transition behavior. The blends exhibit single, composition-dependent glass transition temperatures that accord Braun–Kovacs equation quite well. The crystallization of PEO in the blends was obviously hindered by PPAEK, as shown by the dramatic lowering of the PEO crystallinity and the decrease of PEO crystallization rate. At higher temperatures, the PPAEK/PEO blends underwent phase separation, i.e., the blends display the LCST behavior. A step-heating thermal analysis was designed to determine the phase boundary with DSC. The significant changes in the thermal properties of blends were utilized to judge the mixing status for the blends.

Acknowledgements

We are grateful to the referees for the very helpful comments. The financial support from Ministry of Education, PRC under an Excellent Young Teacher Program (EYTP, Project No. 2066) was acknowledged. One of the authors (K. Nie) would like to thank the support from the Natural Science Foundation of Anhui Province, PRC (Project No. 03044801).

References

[1] O. Olabisi, L.M. Robeson, M.T. Show, Polymer–Polymer Miscibility, Academic Press, New York, 1979.
[2] L.A. Utracki, Polymer Blends and Alloys, Hanser Publisher, New York, 1989.
[3] K.L. Liu, H.C. Zhang, T.L. Chen, Chinese Patent, CN8510117211 (1985).
[4] Q. Guo, J. Huang, B. Li, T. Chen, H. Zhang, Z. Feng, Polymer 32 (1991) 58.
[5] Q. Guo, T. Fang, T. Chen, Z. Feng, Polym. Commun. 32 (1991) 22.
[6] Q. Guo, Eur. Polym. J. 28 (1992) 1049.
[7] Q. Guo, L. Qiu, M. Ding, Z. Feng, Eur. Polym. J. 28 (1992) 1045.
[8] Q. Guo, L. Qiu, M. Ding, Z. Feng, Eur. Polym. J. 28 (1992) 481.
[9] X. Song, S. Zheng, J. Huang, P. Zhu, Q. Guo, J. Appl. Polym. Sci. 79 (2001) 598.
[10] Q. Guo, J. Huang, T. Chen, J. Appl. Polym. Sci. 42 (1991) 2851.
[11] A.J. Kovacs, Adv. Polym. Sci. 3 (1963) 394.
[12] W. Li, R.E. Prud'homme, J. Polym. Sci., Part B: Polym. Phys. Ed. 31 (1993) 719.
[13] S. Zheng, J. Huang, Y. Li, Q. Guo, J. Polym. Sci., Part B: Polym. Phys. Ed. 35 (1997) 1383.
[14] A.R. Schulz, A.L. Young, Macromolecules 13 (1980) 633.
[15] M. Bank, J. Leffingwell, C. Ties, J. Polym. Sci., Part A: Polym. Chem. 10 (1972) 1079.
[16] M.B. Djordjevic, R.S. Porter, Polym. Eng. Sci. 22 (1977) 706.
[17] A. Robard, D. Patterson, G. Delmas, Macromolecules 10 (1977) 706.
[18] E.M. Pearce, T.K. Kwei, B.Y. Min, J. Macromol. Sci., Chem. A21 (1984) 1181.
[19] S. Zheng, J. Huang, J. Li, Q. Guo, J. Appl. Polym. Sci. 69 (1998) 675.
[20] T. Nishi, T.T. Wang, Macromolecules 8 (1975) 809.
[21] R.L. Imken, D.R. Paul, J.W. Barlow, Polym. Eng. Sci. 16 (1976) 593.
[22] X. Li, S.L. Hsu, J. Polym. Sci., Part B: Polym. Phys. 22 (1984) 1331.
[23] T.G. Fox, Bull. Am. Phys. Soc. 1 (1956) 23.
[24] M. Gordon, J.S. Taylor, J. Appl. Chem. 2 (1952) 495.
[25] G. Belorgey, R.E. Prud'homme, J. Polym. Sci., Polym. Phys. Ed. 20 (1982) 191.
[26] G. Belorgey, M. Aubin, R.E. Prud'homme, Polymer 23 (1982) 1051.
[27] M. Aubin, R.E. Prud'homme, Macromolecules 21 (1988) 2945.
[28] Y.W. Cheung, R.S. Stein, Macromolecules 27 (1994) 2512.
[29] G. Braun, A.J. Kovacs, in: J.A. Prins (Ed.), Physics of Non-Crystalline Solids, North-Holland, Amsterdam, The Netherlands, 1965.
[30] D.W. Van Krevelen, P.J. Holftyzer, Properties of Polymer, second ed., Elsevier, Amsterdam, 1980.
[31] A.C. Fernandes, J.W. Barlow, D.R. Paul, J. Appl. Polym. Sci. 29 (1984) 3381.
[32] Y. Li, M. Stein, B.-J. Jungnickel, Colloid Polym. Sci. 269 (1991) 772.
[33] Y. Li, B.-J. Jungnickel, Polymer 34 (1993) 9.
[34] B.-J. Jungnickel, Curr. Trends Polym. Sci. 2 (1997) 157.
[35] H. Lü, S. Zheng, Polymer 44 (2003) 4689.
[36] S. Zheng, S. Ai, Q. Guo, J. Polym. Sci. Part B: Polym. Phys. 41 (2003) 466.